

On electron transport in fast ignition research and the use of few-cycle PW-range laser pulses

J Meyer-ter-Vehn¹, J Honrubia², M Geissler¹, S Karsch¹, F Krausz¹,
G Tsakiris¹ and K Witte¹

¹ Max-Planck-Institute for Quantum Optics, D-85748 Garching, Germany

² ETSII, Universidad Politecnica, Madrid, Spain

Received 1 July 2005

Published 11 November 2005

Online at stacks.iop.org/PPCF/47/B807

Abstract

In this contribution, we address laser-driven electron transport in fast ignition research and the need for ultra-fast (<10 fs) pump–probe diagnostics to study, on the microscopic level, current filamentation and related anomalous energy deposition. Rates of instability growth consistent with realistic fast ignition parameters are discussed. A 3D-hybrid-PIC simulation is presented as an illustrative case. The development of 5 fs PW-range laser pulses at MPQ is reported, which may generate ultra-bright VUV-, x-ray, electron and ion beam pulses to be used for ultra-fast plasma probing.

(Some figures in this article are in colour only in the electronic version)

1. Introduction

Fast ignition of fusion targets (Tabak *et al* 1994) is a most innovative branch of inertial fusion research. It has attracted much attention recently by promising experiments at ILE, Osaka (Kodama *et al* 2002). For a brief overview, one may refer to the book by Atzeni and Meyer-ter-Vehn (2004). The ILE results showed 1000 times enhanced thermonuclear neutron yield due to an ignitor beam providing additional heating to compressed DD fuel. The results exceeded expectations based on numerical simulation. In the experiments spherical CD shells were imploded to densities of 50–100 g cm⁻³. The laser ignitor beam was then guided to the compressed core by means of a metal cone, in which it generated a directed electron beam that heated the fuel to 800 eV. About 20% of laser energy was coupled to the fuel.

The electron transport from cone to fuel involves very high currents and magnetic fields. It is subject to filamentation instability, the nonlinear turbulent stage of which is still poorly understood. Open questions concern beam divergence and anomalous stopping, which may prevent transport to a sufficiently small fuel spot, but may also help energy deposition over a sufficiently short stopping range. Here we consider electron transport involving plasma return currents, filamentation instability and possibly magnetic micro-turbulence and anomalous beam stopping. These phenomena involve dynamics on the time-scale of the inverse plasma

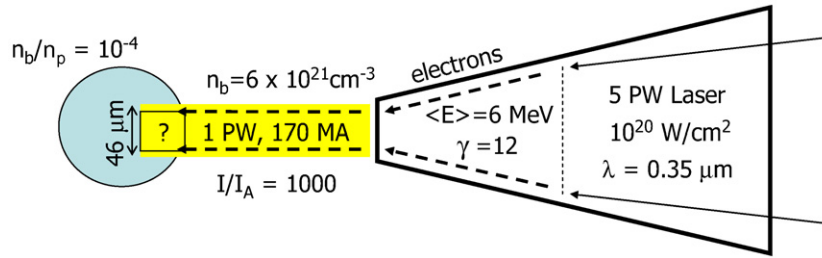


Figure 1. Configuration and parameters for cone-guided fast ignition.

frequency, which is in the range of 10 fs to 100 as, given the high plasma and beam densities. This calls for pump–probe experiments for resolving this time domain. Corresponding probe pulses are now being developed at MPQ and will be briefly described. Such flashlights may allow the observation of the true filamentation patterns, which are not clearly seen in present time-integrated measurements.

2. Parameter set for cone-guided fast ignition

In cone-guided fast ignition, the ignitor beam consists of a relativistic electron pulse generated in a metal cone, as is sketched in figure 1. The energy to be deposited into the spherical fuel volume on the left has been studied by Atzeni (1999). Choosing compressed fuel of 1300 times liquid DT density, at least 1 PW (10^{15} W) ignitor power is required, corresponding to 24 kJ of energy deposited within 24 ps into a cylindrical fuel volume of $46 \mu\text{m}$ diameter.

The deposition depth is a matter of concern. It depends on the relativistic γ -factor of the beam electrons as well as on the stopping mechanism. The beam energy spectrum typically has an exponential shape with an effective temperature of

$$T_{\text{eff}} \approx \langle \gamma \rangle mc^2 = f mc^2 a_0, \quad (1)$$

where $mc^2 = 511 \text{ keV}$ and $a_0 = eA_0/mc^2$ is the normalized light amplitude related to light intensity I and wavelength λ by $I\lambda^2 = 1.37 \times 10^{18} (\text{W cm}^{-2})\mu\text{m}^2 a_0^2$. Though the scaling $\sim a_0 \sim I^{1/2}$ is well confirmed by simulations and experiments, the front factor is less clear, because it depends on target plasma and pulse duration. A general discussion is given by Pukhov *et al* (1999). For normal incidence on an unperturbed solid target, $f \approx 1$ appears adequate, as proposed originally by Wilks *et al* (1993). Also the 3D-PIC simulation of a cone configuration by Sentoku *et al* (2004) supports this value for the electron spectrum after 50 fs of irradiation. However, for the 24 ps irradiation required for fast ignition, we expect substantial ablation to occur from the cone surface, and the spectra will become more energetic. For gradient lengths of $50 \mu\text{m}$ and larger, one obtains $f \approx 3$ (Pukhov *et al* (1999), see figure 2), and this value is used in the following. In the example of figure 1, we have estimated an effective electron energy of $\langle E \rangle = 6 \text{ MeV}$ arising from an 5 PW incident laser pulse having $\lambda = 0.35 \mu\text{m}$ and $I = 10^{20} \text{ W cm}^{-2}$.

Taking a 20% laser-to-electron conversion efficiency, we arrive at 1 PW electron power and a total electron current of 170 MA. This corresponds to 1000 times the Alfvén current $J_A = 17 \text{ kA}$, $\gamma \approx 170 \text{ kA}$. In vacuum, transport of currents exceeding the Alfvén limit is inhibited by self-generated magnetic fields. In plasma, larger currents can propagate provided that induced plasma currents reduce the net current and the corresponding B -fields.

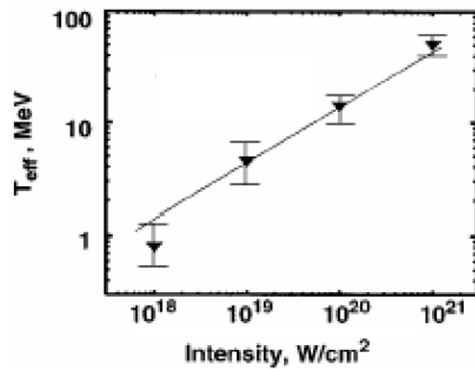


Figure 2. Effective electron temperature as obtained from 3D-PIC simulation (Pukhov *et al* 1999) versus laser intensity for an exponential density profile of $30\ \mu\text{m}$ scale length, which is cut off at critical density. The straight line corresponds to equation (1) and $f \approx 3$.

In fact, the beam current generates such plasma return currents trying to prevent magnetic field build-up. But this configuration of counter-propagating currents is subject to transverse filamentation instability and longitudinal two-stream instability. The system then decays into complex time-dependent patterns of small-scale current filaments and electromagnetic fields. In the strongly driven case prevalent in fast ignition applications, it may lead to a regime of magnetic turbulence which causes anomalous beam stopping significantly larger than classical stopping due to binary collisions. These regimes may become of central importance for fast ignition research. We are just beginning to explore the underlying physics and the consequences for energy transport. In the following, we briefly review the present status of understanding and discuss possibilities to investigate the dynamics on femto-to-attosecond scales, using new few-cycle lasers.

3. Current filamentation and anomalous beam stopping

In the context of fast ignition, current filamentation has been studied by Honda *et al* (2000) on the basis of collisionless 2D-PIC simulation. A typical result is reproduced in figure 3, showing the decay of an initially uniform system of relativistic electron beam and compensating plasma return currents with zero net current. A beam-to-plasma density ratio of 0.1 was chosen. The uniform beam decays on the time-scale of the inverse plasma frequency into a large number of beam filaments (spots) which, in a later non-linear phase, attract each other and merge. Each event of filament coalescence is accompanied by beam energy dissipation. This is seen in figure 3(b) as jumps in the forward directed power flow. As a rule, the plasma return current is almost completely pushed out of the beam filaments which then carry a current of about one Alfvén current. The beam energy loss caused by these collective plasma dynamics is about 1000 times larger than losses due to binary collisions. Qualitatively, these 2D-PIC results have been confirmed in 3D-PIC simulations performed by Sentoku *et al* (2003).

Unfortunately, the results discussed above apply only to the low density part of the imploded fuel configuration. PIC simulations have to resolve the microscopic plasma scales (ω_p^{-1} in time and c/ω_p in space) and are still not feasible for full fast ignition simulations including the high density parts. Also plasma resistivity, typically not modelled in PIC, will affect the return currents. In order to overcome these limitations hybrid codes have been developed. They make use of PIC only for the beam, but treat the plasma background in

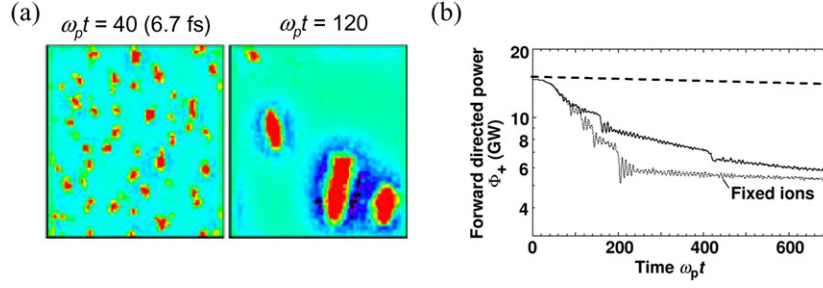


Figure 3. (a) Transverse cuts (x, y plane) through electron beam current (spots), (b) beam power in z direction versus time; the broken line indicates the level of classical Coulomb stopping (see text, and Honda *et al* (2000)).

a resistive MHD approximation (Taguchi *et al* 2001 and 2004). Even simpler macroscopic modelling (Bell *et al* 1997, Gremillet *et al* 2002, Welsh *et al* 2004, Honrubia *et al* 2005) for treating resistive filamentation is based on Maxwell's equations (dropping $\partial E/\partial t$) and Ohm's law alone:

$$\begin{aligned} j_p &= -j_b + (1/\mu_0)\nabla \times B, \\ E &= \eta j_p, \\ \partial B/\partial t &= -\nabla \times E. \end{aligned} \quad (2)$$

Here, the total current density $j = j_b + j_p$, consisting of beam and plasma component, determines the B -field, and the E -field is obtained from Ohm's law using a macroscopic plasma resistivity $\eta(T)$; essentially, it only depends on local temperature. Hydrodynamics and electrostatic fields due to charge separation are neglected in the simplest version of this approach. But it models plasma return currents, beam stopping due to resistive E -fields, and energy deposition in the plasma due to Ohmic heating:

$$\varepsilon = j_p \cdot E = \eta j_p^2. \quad (3)$$

The linear stability of a relativistic electron beam with respect to resistive filamentation has been studied within this model by Gremillet *et al* 2002. The growth rate depends on the beam parameters: γ -factor $\gamma_b = 1/(1 - \beta_b^2)^{1/2}$, transverse thermal velocity $\beta_{tb} = v_{tb}/c$, the beam plasma frequency ω_b and the magnetic diffusion time $\tau_d = \mu_0 c^2/(\eta\omega_b)$. The dispersion relation is

$$\tilde{\Gamma} \tau_d + \kappa^2 + \frac{1}{\gamma_b^3} + \frac{1}{\gamma_b} \left(\frac{\beta_b}{\beta_{tb}} \right)^2 Z' \left(\frac{i\tilde{\Gamma}}{\kappa\beta_{tb}} \right) = 0, \quad (4)$$

containing the plasma dispersion function Z . The growth rate $\tilde{\Gamma} = \Gamma/\omega_b$ as a function of wave number $\kappa = kc/\omega_b$ is plotted in figure 4 for various beam parameters and resistivities. It is found that typical growth rates are in the order of ω_b , corresponding to times to the order of 1–100 fs. One should notice that the beam densities can be well beyond the laser critical density (compare figure 1) because of electron beam compression in the cone and magnetic pinching during transport.

4. 3D-hybrid-PIC simulation

Here we report on a simulation using a 3D-hybrid-PIC code based on this model (Honrubia *et al* 2005) and treating high densities realistic for FI. The intention is to demonstrate

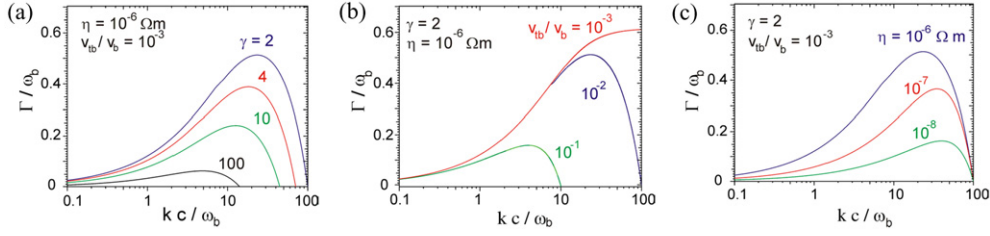


Figure 4. Growth rates of filamentation instability in units of beam plasma frequency versus wave number for uniform plasma and beam and (a) different beam γ -value, (b) different transverse beam temperature and (c) different resistivity values.

that filamentation and anomalous stopping also show up under these conditions. Similar simulations based on a 2D-hybrid-PIC code (Welsh *et al* 2004) were reported recently by Campbell *et al* (2005), however, without discussing the underlying physics in detail.

In figures 5 and 6, results are shown for a 1 GA, 1 PW beam with monoenergetic electrons of $(\gamma_b - 1)mc^2 = 1$ MeV, transverse temperature $T_{\perp} = 120$ keV and angular spread of 30° . The beam is injected into DT plasma with exponential density profile rising from 2 to 100 g cm^{-3} over a distance of $50 \mu\text{m}$. Plasma resistivity is modelled according to Spitzer. One observes strong beam filamentation. It leads to anomalous collective energy deposition (see figures 6(a) and (b)), which now exceeds classical stopping only by a factor of 3 rather than by the factor of 1000 obtained by PIC for lower densities (see section 3). Within the present simulation, energy deposition can only occur due to binary collisions of beam electrons and due to Ohmic heating. Both contributions are given in figure 6(b). One should notice that the Ohmic heating is enhanced due to filamentation. The enhancement relative to equation (3) is given by

$$\varepsilon_{\text{coll}} = \langle \eta(j_p^2 - \langle j_p \rangle^2) \rangle, \quad (5)$$

where $\langle \dots \rangle$ denotes averaging over the beam cross-section. Apparently, transverse current fluctuations lead to additional *collective* energy deposition. This increases, effectively, resistivity and E -field, and thereby it leads to anomalous beam stopping. Corresponding high temperatures up to 30 keV show up in the low-density part of figure 5(a). Since this reduces resistivity ($\sim T^{5/2}$), energy deposition self-regulates, and actually most beam energy is deposited into the higher density regions as is evident from figure 6(a). One should notice that the beam filaments originating from the low-density side may carry beam densities higher than at the point of injection and that filamentation may play a significant role also in the dense fuel regions.

The present findings are indicative only. Apparently, very complex dynamics govern the energy transport in fast ignition and require adequate experimental investigation. Possibilities of pump-probe diagnostics allowing for femtosecond time resolution are briefly discussed in the following section.

5. Generation of few-cycle PW pulses

The generation of a 8 mJ laser pulse with pulse duration of less than 10 fs and power above 1 TW has been demonstrated at MPQ using OPCPA techniques (Ishi *et al* 2005). Lasers with powers up to 1 PW (5 J, 5 fs) are presently under development and are expected to become available for experiments soon (Krausz *et al* 2005). These pulses will allow the generation of ultra-bright electron (Pukhov and Meyer-ter-Vehn 2002, Faure *et al* 2004), ion and x-ray pulses of same pulse duration. Via harmonic generation on plasma surfaces (Lichters *et al* 1997), they may

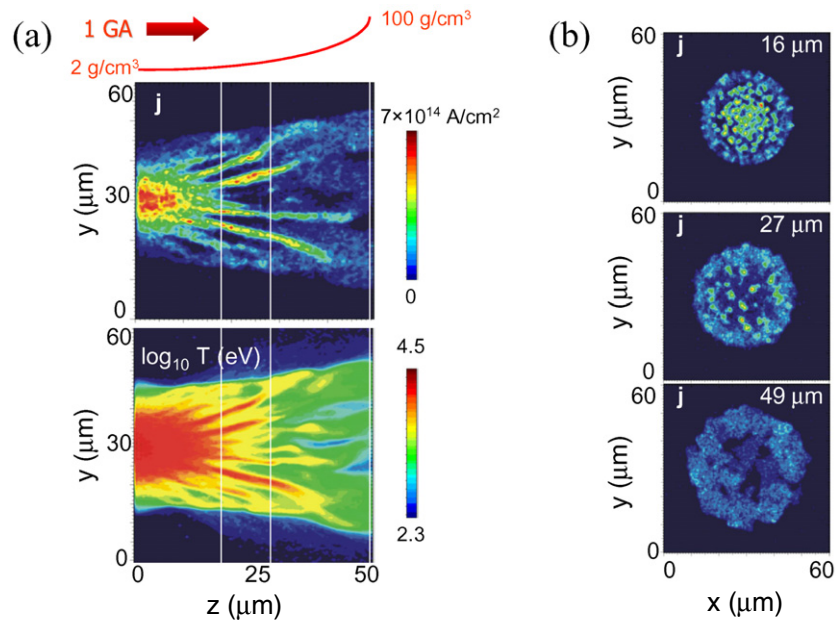


Figure 5. 3D-hybrid-PIC simulation showing a continuous 1 GA beam of 1 MeV electrons with 120 keV transverse temperature injected into plasma with density rising exponentially from 2 to 100 g cm^{-3} after 1.2 ps. (a) Longitudinal y, z cuts showing beam current density and temperature and (b) transverse x, y cuts at different z positions and 1.2 ps.

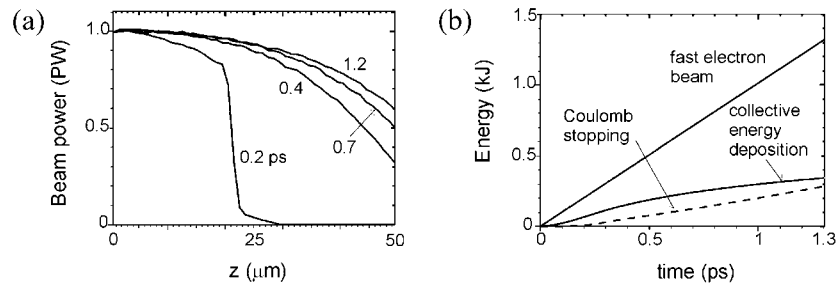


Figure 6. (a) Beam power versus penetration depth at different times, (b) partition of various energy components as a function of time; same simulation as given in figure 5.

also produce electromagnetic spikes of 10 as duration and less (Gordienko *et al* 2004). We envision experiments in which a major part of a few-cycle PW pulse is used for generating a 100 TW electron pulse driving a 1–10 MA current in dense plasma and to time-resolve current filaments with synchronized attosecond x-ray pulses. This is sketched schematically in figure 7.

6. Conclusions

We have discussed aspects of high-current electron transport in fast ignition research, indicating regimes of magnetic turbulence due to filamentation instability and corresponding anomalous collective beam deposition. This may explain the high laser-to-fuel coupling observed in

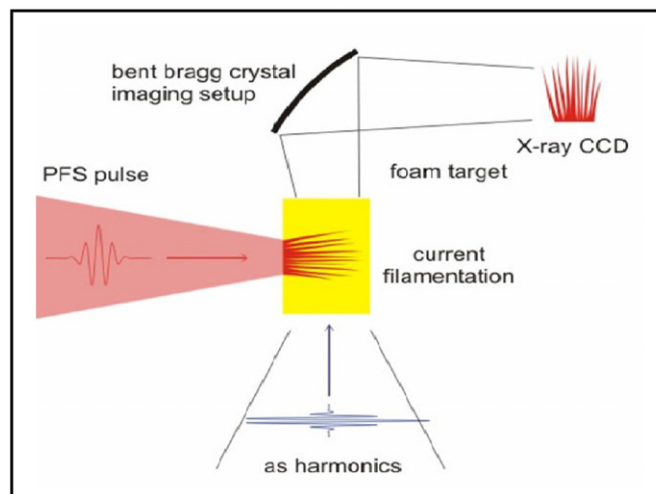


Figure 7. Schematic configuration of a pump-probe experiment exploring relativistic electron transport and current filamentation with few-cycle PW-range pump pulses and attosecond probe pulses.

cone-guided fast ignition experiments. Direct observation of the turbulent regime requires pump-probe diagnostics with femtosecond time resolution, which may become possible with the new development of few-cycle PW-range laser pulses.

Acknowledgment

This work was supported by EURATOM within IFE keep-in-touch activities.

References

- Atzeni S 1999 *Phys. Plasmas* **6** 3316
 Atzeni S and Meyer-ter-Vehn J 2004 *The Physics of Inertial Fusion* (Oxford: Clarendon)
 Bell A R, Davies J R, Guerin S and Ruhl H 1997 *Plasma Phys. Control. Fusion* **39** 653
 Campbell R B *et al* 2005 *Phys. Rev. Lett.* **94** 055001
 Faure J *et al* 2004 *Nature* **431** 541
 Gordienko *et al* 2004 *Phys. Rev. Lett.* **93** 115002
 Gremillet L, Bonnaud G and Amiranoff F 2002 *Phys. Plasmas* **9** 941
 Honda M, Meyer-ter-Vehn J and Pukhov A 2000 *Phys. Rev. Lett.* **85** 2128
 Honrubia J *et al* 2005 *Phys. Plasmas* **12** 052702
 Ishi N *et al* 2005 *Opt. Lett.* **30** 567
 Kodama R *et al* 2002 *Nature* **418** 933
 Krausz F *et al* 2005 *PW Field Synthesizer* (PFS., MPQ project study)
 Pukhov A, Sheng Zh-M and Meyer-ter-Vehn J 1999 *Phys. Plasmas* **6** 2847
 Pukhov A and Meyer-ter-Vehn J 2002 *Appl. Phys. B* **74** 355
 Sentoku Y, Mima K, Kaw P and Nishikawa K 2003 *Phys. Rev. Lett.* **90** 155001
 Sentoku Y *et al* 2004 *Phys. Plasmas* **11** 3083
 Tabak M *et al* 1994 *Phys. Plasmas* **1** 1626
 Taguchi T, Antonsen T M and Mima K 2004 *Comput. Phys. Commun.* **164** 269
 Welsh D R *et al* 2004 *Comput. Phys. Commun.* **164** 183